Journal of Forensic Radiology and Imaging 7 (2016) 21–27

Contents lists available at ScienceDirect

Journal of Forensic Radiology and Imaging

journal homepage: www.elsevier.com/locate/jofri

A novel method for landmark-based personal identification on panoramic dental radiographic and computed tomographic images

Hideko Fujimoto[a,b,*], Takeshi Hayashi[b], Morio Iino[b]

[a] Kyoto Forensic Odontology Center, Fujimoto Clinic for Oral and Maxillofacial Surgery, 664-21 Higashinotoin-dori, Shijo-agaru-nishiiru, Nakagyo-ku, Kyoto 604-8143, Japan

[b] Division of Legal Medicine, Tottori University Faculty of Medicine, 86 Nishicho, Yonago, Tottori 683-8503, Japan

ARTICLE INFO

Keywords:
Personal identification
Panoramic CT
Panoramic X-ray
Landmark method
Procrustes analysis
Forensic odontology

ABSTRACT

Personal identification based on dental work is a well-known and useful method for post-mortem identification. Recently, several odontologists have matched reconstructed post-mortem computed tomographic (CT) panoramic images of unidentified bodies with ante-mortem dental panoramic X-ray images for identification purposes. However, it is not always possible to obtain useful information from these panoramic X-ray and CT images. To obtain more accurate information for personal identification, we focused on the anatomical structures of the maxilla and mandible rather than dental work on the images.

The aim of the present research is to develop a novel method for the personal identification of unidentified bodies, based on landmarks on the tooth sockets, which are not notably subject to post-mortem changes. We calculated the Procrustes distance and Pearson's correlation coefficients of the landmarks of two sample images, and used the results to correctly identify the subjects from among a pool of 100 candidates, without having to rely on information on dental work. We conclude that this method is a reliable tool and can be easily and rapidly applied for victim and missing person identification.

1. Introduction

Dental panoramic X-ray images are commonly provided by clinical dentists to odontologists as ante-mortem (AM) dental information for police investigations [1]. Computed tomography (CT) images are not as popular as X-ray images for AM dental information because they are not often obtained by clinical dentists [2]. However, post-mortem (PM) CT imaging has recently been widely used in forensic field and clinical hospitals [1]. The identification process typically involves the matching of dental work on the images of victims [2].

Several studies have examined the use of intraoral X-ray images for victim identification [3–11]. However, a number of limitations have been encountered in victim identification that focuses on dental work alone. These include (1) insufficient information about the dental work due to the body being in a less-than-ideal condition; (2) misleading information owing to errors and deficiencies in the AM dental records; and (3) lack of dental work in some cases.

Recently, increasing attention has been paid to the use of anatomical structures on the images for identification purposes [12,13].

On the other hand, CT scanning provides more complete PM data, and can be used on bodies in a variety of conditions. By using CT images, we can not only obtain information about the dental work, but also anatomical information about the jaw, including the tooth sockets, through easy operations performed using common imaging software [14,15].

In the present study, we evaluated whether AM dental panoramic X-ray images and “post-mortem” CT (“PM” CT) panoramic images could serve as suitable data for matching using the anatomical structures and not using dental work characteristics for personal identification.

The aim of this study is to develop a novel method in victim identification that is to prepare for Disaster Victim Identification system (DVI) and to aid in the search for missing persons among those with search requests.

2. Materials and methods

2.1. Research participants

A total of 100 volunteer patients (50 female and 50 male) from the Fujimoto Clinic for Oral and Maxillofacial Surgery (Kyoto, Japan; female subjects ranging from 12 years to 73 years [average age 35

* Corresponding author at: Kyoto Forensic Odontology Center, Fujimoto Clinic for Oral and Maxillofacial Surgery, 664-21 Higashinotoin-dori, Shijo-agaru-nishiiru, Nakagyo-ku, Kyoto 604-8143, Japan.
E-mail address: kyoto.f.o@gmail.com (H. Fujimoto).

http://dx.doi.org/10.1016/j.jofri.2016.10.002
Received 11 April 2016; Received in revised form 13 September 2016; Accepted 23 October 2016
Available online 24 October 2016

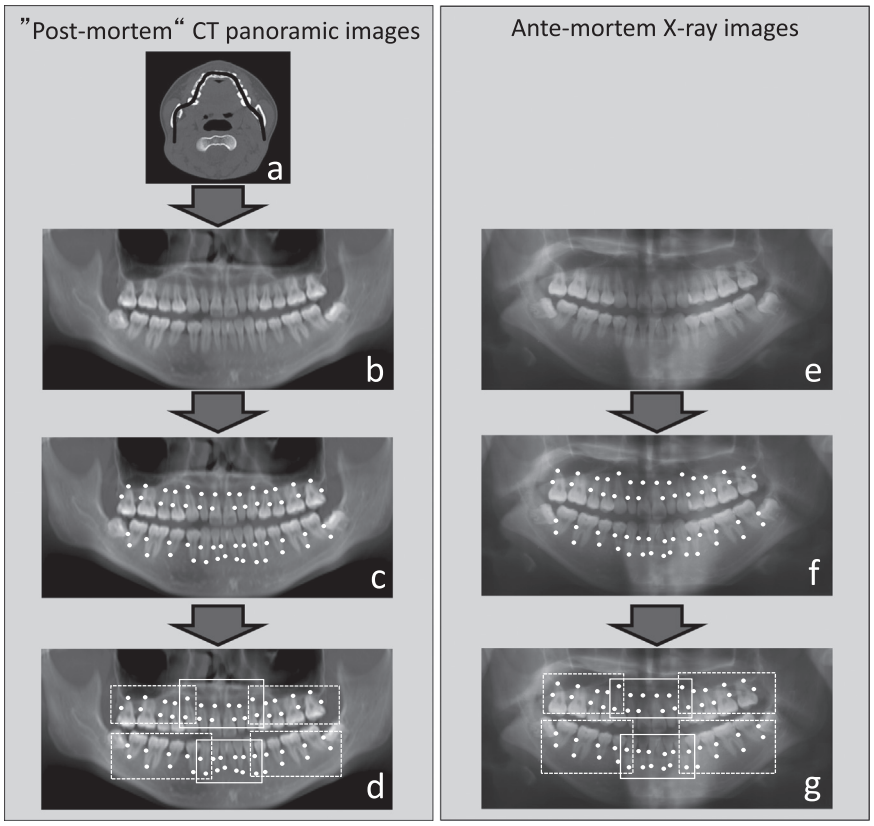

Fig. 1. Workflow process of measurement of the ante-mortem and “post-mortem” images The “PM”CT panoramic image (Fig. 1b–d) was reconstructed from the MPRCT images by drawing the line along the teeth (Fig. 1a). A representative AM images (Case 33) are shown on the right (Fig. 1e–g). The Landmarks (white dots) were marked on each image on the distal alveolar ridge and the bottom of distal or single root socket of the teeth except the wisdom tooth (Fig. 1c, f). Then every image was divided into 6 segments (Fig. 1d, g).

years] and male subjects from 12 years to 83 years [average age 43 years]) participated in our study. The 100 patients ranged in age from 12 years to 83 years (average 39 years).

2.2. “Post-mortem” data

The dental CT images of 2 out of the 100 patients (Sample A and B) were chosen to represent the “PM” data.

2.3. Ante-mortem data

We used all 100 patients’ clinical X-ray data to create a pool of unidentified AM data. We obtained informed consent to use the dental panoramic X-ray images of the patients’ jaws. All of the images had been obtained at the clinic prior to the present study for therapeutic purposes and not for the purposes of this study.

Sample A is a case of 18-year-old female patient with progenia. She had undergone a CT scan 29 days after the dental panoramic X-ray in preparation for a mandibular osteotomy (Intraoral Vertical Ramus Osteotomy; IVRO), for the purposes of mandibular correction. She had 30 teeth sockets.

Sample B is a case of 53-year-old male patient with maxillary atrophy. His CT scan was performed 40 days after the dental panoramic X-ray, in preparation for a vestibule plastic operation with skin graft. He had 12 teeth sockets. These two cases had few dental works, and one (Sample A) had a large number of teeth sockets, while the other (Sample B) had fewer teeth sockets. These patients agreed to provide the CT images of their jaws for the study. All of the images were obtained prior to the present study for therapeutic purposes.

2.4. Workflow process

We collected dental panoramic X-ray films of the maxillae and the mandibles of 100 patients (Cases 1-100) to serve as the AM data. All of the X-ray images were obtained and filmed at our clinic using the same dental panoramic X-ray equipment (PM2002C, Planmeca Oy, Helsinki, Finland) from September 2005 to February 2014 by a single dentist (Doctor of Medical Dentistry: DMD).

We digitized the films into Joint Photographic Experts Group (JPEG) images using a film scanner (GT-9800F, Seiko Epson Corporation, Nagano, Japan). A representative AM image (Case 33) is shown on Fig. 1e. All of the films were anonymized so that the researcher (a board-certified forensic odontologist; H.F., DMD) was blinded to the names of the patients.

The CT images of the jaws of Samples A and B were scanned by a licensed radiographer using a multidetector row CT scanner (Aquilion 16, Toshiba Medical Systems, Tochigi, Japan). The thickness of the slices was 1 mm, with a collimation of 16×1.0 mm. The images were saved as the “PM” data (Figs. 1a, 2a, 3a).

The “PM”CT panoramic images were reconstructed from the CT images by using dental imaging software (OnDemand3D, Cybermed, Seoul, Republic of Korea) on a PC running Microsoft Windows 7 (Figs. 1b, 2b, 3b). We used the Curved Multi Planar Reconstruction (CPR) dental mode with settings of 0.1 mm for the cross-interval, 0.1 mm for the panorama interval, and 30 mm for the thickness. Two landmarks were marked: on the distal alveolar ridge and on the bottom of the distal or single root socket of every tooth, except for the wisdom teeth (Fig. 1c, f). There was a maximum of 28 teeth and 56 landmarks because humans typically have 28 teeth, not counting the wisdom teeth. None of the artificial tooth sockets made for dental treatments received a landmark.

Calculations involving 28 segments (i.e., the natural number of

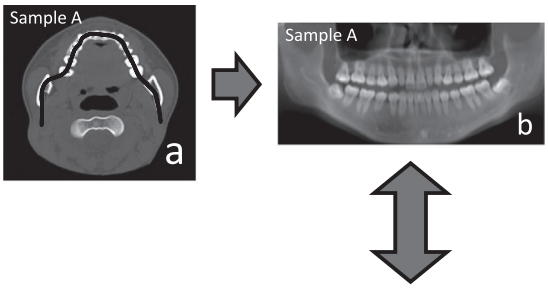

Ranking Case No.	Procrustes D. R	Ante-mortem X-ray images
1st place 33	0.68245 0.99636	c
2nd place 11	0.92507 0.99331	d
3rd place 13	0.95454 0.99288	e
4th place 57	1.00935 0.99204	f
5th place 5	1.01296 0.99198	g

Fig. 2. "PM" CT panoramic image (Sample A) with matched/unmatched AM dental panoramic X-ray images The five best matches among the AM data are shown on Fig. 2c–g. Case 33 had the highest matching score of Procrustes distance and correlation coefficients (Fig. 2c). Case 11, 13 57 and 5 were eliminated because of the wisdom tooth (Fig. 2d–g).

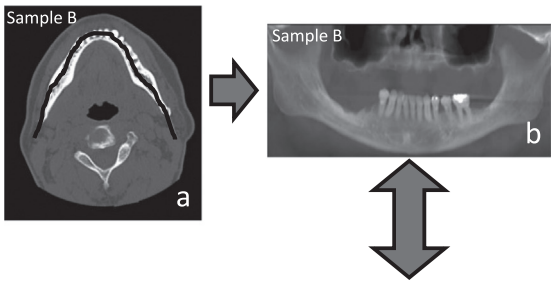

Ranking Case No.	Procrustes D. R	Ante-mortem X-ray images
1st place 87	0.57481 0.99410	c
2nd place 62	0.77528 0.98927	d
3rd place 5	0.80637 0.98839	e
4th place 21	0.83839 0.98745	f
5th place 32	0.84122 0.98736	g

Fig. 3. "PM" CT panoramic image (Sample B) with matched/unmatched AM dental panoramic X-ray images The five best matches among the AM data are shown on Fig. 3c–g. Case 87 had the highest matching score of Procrustes distance and correlation coefficients (Fig. 3c). Case 62, 21 and 32 were eliminated because of the dental works (Fig. 3d, f, g). Case 5 was eliminated because of the alveolar bone absorption (Fig. 3e).

teeth) would have been complicated and time-consuming. Therefore, we attempted to simplify the process by dividing each image of the jaws into fewer segments. We first used a 2-segment method to divide the image into the maxilla and mandible. We compared the results with a 4-segment method that divided the image into the right and left segments of the maxilla and mandible, with each segment sharing one overlapping tooth with the next segment.

Next we attempted to divide the image into six segments, i.e., the right, middle and left segments of the maxilla and the mandible (Fig. 1d, g). The right maxilla/mandible segment included the following five teeth: the right second molar, right first molar, right second pre-molar, right first pre-molar and right canine. The middle maxilla/mandible segment included the following six teeth: the right canine, right lateral incisor, right central incisor, left central incisor, left lateral incisor, and left canine. The left maxilla/mandible segment included the remaining 5 teeth. Each segment shared one overlapping tooth with the next segment.

For each segment, the x and y coordinates of the landmarks were recorded. The coordinates were measured using image manipulation software (GIMP 2.8.0, GIMP shop, The GIMP Development Team) on a PC running Microsoft Windows 7. Each image had a maximum of 56 data points. Procrustes analysis was performed on each segment for statistical shape analyses [4]. To optimally superimpose the maxilla/mandible records from each "PM" sample with the candidate AM data, the data points were allowed to be freely translated, rotated, and scaled. We performed calculations within each segment followed by an overall score.

To quantify the anatomical similarities between each sample and the candidates, the Procrustes distances and Pearson's correlation coefficients between the sample's data points and the corresponding points of the candidates were calculated with the following equations, using Microsoft Excel 2010 (Microsoft Corporation, Redmond, WA, USA).

$$r = \frac{\sum_{i=1}^{n} f_i g_i}{\sqrt{\sum_{i=1}^{n} f_i^2}\sqrt{\sum_{i=1}^{n} g_i^2}} \qquad d = \sqrt{\sum_{i=1}^{n} (f_i - g_i)^2}$$

The equations are the formulae for Pearson's correlation coefficient (r) and the Procrustes distance (d); f_i and g_i are the sets (N=112) of landmarks for comparison. The five best matches among the AM data were extracted for testing via final visual examination (Tables 1, 2). The entire process was performed separately for Sample A and Sample B.

Table 1
Result of Procrustes distance and correlation coefficient.
Sample A.

Case No.	Age	Procrustes D. R.	Case No.	Age	Procrustes D. R.	Case No.	Age	Procrustes D. R.	Case No.	Age	Procrustes D. R.
1	21		26	23	1.42933 0.98404	51	25	1.30650 0.98667	76	53	
2	28	2.24492 0.96063	27	46	1.25733 0.98765	52	25	1.13679 0.98990	77	25	
3	27	1.27978 0.98720	28	26	1.20342 0.98869	53	27		78	57	
4	25		29	42	1.34896 0.98578	54	33	1.03511 0.99163	79	20	1.41508 0.98436
5	22	**1.01296** **0.99198**	30	27	1.42036 0.98424	55	32	1.20556 0.98865	80	18	1.27171 0.98737
6	18		31	30	1.55208 0.98118	56	24		81	19	1.14639 0.98973
7	35	1.60106 0.97997	32	41	1.26458 0.98751	**57**	23	**1.00935** **0.99204**	82	66	
8	27	1.33058 0.98617	**33**	18	**0.68245** **0.99636**	58	26	1.04336 0.99150	83	53	
9	20	1.03318 0.99166	34	44	1.15093 0.98965	59	53	1.27828 0.98723	84	52	
10	59	1.00303 0.99214	35	40	1.50436 0.98232	60	38	1.43492 0.98391	85	61	
11	37	**0.92507** **0.99331**	36	37	1.02474 0.99180	61	60		86	63	
12	31	1.21716 0.98843	37	65		62	47	1.06993 0.99106	87	53	
13	34	**0.95454** **0.99288**	38	19		63	60		88	55	
14	22	1.23574 0.98807	39	56		64	42	1.21790 0.98841	89	56	
15	28	1.11698 0.99025	40	44		65	28	1.03994 0.99155	90	12	1.35606 0.98563
16	25	1.16185 0.98945	41	36		66	31	1.22563 0.98826	91	42	1.42652 0.98410
17	32	1.20078 0.98874	42	73		67	33	1.18507 0.98903	92	56	1.26011 0.98760
18	33	1.14169 0.98982	43	45		68	62	1.30151 0.98677	93	63	
19	73		44	35		69	22	1.44060 0.98379	94	43	
20	22	1.23596 0.98807	45	12		70	27	1.08591 0.99079	95	38	1.43195 0.98398
21	30	1.05528 0.99130	46	31	1.37570 0.98521	71	20	1.17430 0.98923	96	67	
22	45	1.18052 0.98911	47	16	1.31870 0.98641	72	23	1.09652 0.99061	97	62	
23	35	1.30494 0.98670	48	34		73	53		98	42	
24	29	1.52432 0.98185	49	51	1.41314 0.98440	74	60		99	83	
25	22	1.09439 0.99064	50	57		75	50		100	70	

The patients (Cases 1,4, 6, 19, 37–45, 48, 50, 53, 56, 61, 63, 73–78, 82–89, 93, 94 and 96–100) were excluded from the process of calculating Procrustes distance and correlation

The visual examination was performed to exclude the AM images that did not match each "PM" sample by a board-certified odontologist (H.F., DMD). One case was selected as the identity of each sample.

3. Results

3.1. Sample A (Fig. 2) (Table 1)

The Procrustes distance values ranged from 0.68245 to 2.24492. Case 33 exhibited the shortest Procrustes distance. The correlation coefficient values ranged from 0.96063 to 0.99636. We extracted five cases (Cases 5, 11, 13, 33 and 57) that ranked within the top 5% in the trial for testing by final visual examination. Four of the five cases (Cases 5, 11, 13 and 57) were eliminated by visual examination due to distinct differences in the wisdom teeth (Fig. 2).

3.2. Sample B (Fig. 3) (Table 2)

The Procrustes distance values ranged from 0.57481 to 1.77742. Case 87 exhibited the shortest Procrustes distance. The correlation coefficient values ranged from 0.94358 to 0.99410. We extracted five cases (Cases 5, 21, 32, 62 and 87) that ranked within the top 5% in the trial for testing by final visual examination. Four of the five cases (Cases 5, 21, 32 and 62) were eliminated by visual examination due to distinct differences in terms of the dental works and the alveolar bone absorption (Fig. 3).

Based on the statistical shape analysis and visual examination, we eventually chose Case 33 as the identity of Sample A and Case 87 as the identity of Sample B. We confirmed that we had matched the correct cases.

Table 2
Result of Procrustes distance and correlation coefficient
Sample B.

Case No.	Age	Procrustes D. R.	Case No.	Age	Procrustes D. R.	Case No.	Age	Procrustes D. R.	Case No.	Age	Procrustes D. R.
1	21	0.88873 0.98589	26	23	1.22182 0.97334	51	25	1.50949 0.95931	76	53	1.19644 0.97444
2	28	1.77742 0.94358	27	46	1.16447 0.97579	52	25	1.11665 0.97773	77	25	
3	27	0.96117 0.98350	28	26	0.88132 0.98613	53	27		78	57	
4	25		29	42	1.21463 0.97366	54	33	1.03073 0.98103	79	20	1.35540 0.96719
5	22	**0.80637** **0.98838**	30	27	1.24830 0.97217	55	32	0.85713 0.98688	80	18	1.48455 0.96065
6	18		31	30	1.16497 0.97577	56	24		81	19	0.97574 0.98300
7	35	1.29278 0.97015	**32**	41	**0.84122** **0.98736**	57	23	1.14383 0.97664	82	66	
8	27	1.30364 0.96965	33	18	1.30152 0.96975	58	26	1.14160 0.97673	83	53	
9	20	0.96423 0.98340	34	44	1.17162 0.97548	59	53	1.10155 0.97833	84	52	1.63480 0.95228
10	59	0.99743 0.98224	35	40	1.40591 0.96470	60	38	1.28587 0.97047	85	61	
11	37	1.01644 0.98155	36	37	1.30797 0.96945	61	60		86	63	
12	31	1.11919 0.97763	37	65		**62**	47	**0.77528** **0.98927**	**87**	53	**0.57481** **0.99410**
13	34	0.99327 0.98238	38	19	1.21176 0.97378	63	60		88	55	
14	22	1.09318 0.97866	39	56		64	42	1.10555 0.97817	89	56	1.00080 0.98211
15	28	0.95645 0.98366	40	44		65	28	1.03468 0.98088	90	12	1.30512 0.96958
16	25	1.04059 0.98066	41	36		66	31	1.30538 0.96957	91	42	1.39630 0.96519
17	32	0.84296 0.98731	42	73		67	33	1.20427 0.97410	92	56	1.29795 0.96992
18	33	0.89990 0.98554	43	45	0.99447 0.98234	68	62	1.18451 0.97495	93	63	1.13327 0.97707
19	73	0.98557 0.98266	44	35		69	22	1.19832 0.97436	94	43	
20	22	1.22163 0.97335	45	12		70	27	1.18832 0.97478	95	38	1.48293 0.96073
21	30	**0.83839** **0.98745**	46	31	1.18558 0.97490	71	20	1.08497 0.97898	96	67	0.95905 0.98358
22	45	1.05547 0.98011	47	16	1.15175 0.97631	72	23	1.08374 0.97903	97	62	1.00538 0.98195
23	35	1.33108 0.96836	48	34	1.19872 0.97434	73	53		98	42	
24	29	1.18843 0.97478	49	51	1.19283 0.97459	74	60	1.61937 0.95317	99	83	
25	22	0.88372 0.98605	50	57		75	50	1.27095 0.97116	100	70	

The patients (Cases 4, 6, 37, 39–42, 44, 45, 50, 53, 56, 61, 63, 73, 77, 78, 82, 83, 85, 86, 88, 94 and 98–100) were excluded from the process of calculating Procrustes distance and

3.3. Six-segment method (Table 3)

There were few numeric differences between two methods (2-segment method and 4-segment method); therefore, it was difficult to evaluate the precision of these division methods. The results of five cases (Cases 5, 11, 13, 33 and 57) that ranked within the top 5% in this trial are presented in Table 3. Consequently, we used the positional relationships (6-segment method), which proved to be precise and effective.

4. Discussion

This study shows that Procrustes distance analysis of the tooth sockets provides a reliable method to objectively identify matching pairs of dental panoramic X-ray images. Our key findings were that the tooth sockets helped a personal identification and Procrustes distance analysis proved to obtain an accurate result quickly.

It should be important to identify with the objective proof. In particular, it can be used for the cases with few dental works and several missing teeth.

For Sample A, we correctly identified the subjects, even without information on dental work. It had 28 teeth sockets to calculate, so that Procrustes distance analysis was made use of the maximum.

For Sample B, which had only 12 tooth sockets, we were also able to select the correct subject. It should be noted that the Procrustes distance values were relatively distinct.

While we are confident that this method is useful, especially for cases with little or no dental work, it does have a few limitations. First, it might not produce accurate results for subjects with only a few remaining tooth sockets. Second, large metallic prostheses would create streak artefacts on CT images, which might hinder the reconstruction process. Third, in cases of severe periodontal disease invol-

Table 3
Result of Procrustes distance and correlation coefficient in the trial.
Sample A.

Case No.	Procrustes D. R.		
	2-segments method	4-segments method	6-segments method
33	**0.41766**	**0.51202**	**0.68245**
	0.99797	**0.99795**	**0.99636**
5	0.57835	0.73976	1.01296
	0.99592	0.99573	0.99198
11	0.46518	0.78333	0.92507
	0.99736	0.99521	0.99331
13	0.59494	0.73145	0.95454
	0.99568	0.99582	0.99288
57	0.55875	0.79669	1.00935
	0.99637	0.99504	0.99204

ving alveolar bone resorption and orthodontic treatment, the structure of the jaw can change over time, which would affect the accuracy of our method. Lastly, if the CT images are unclear, because of damage to the jaws or other reasons, the landmarks might not be placed correctly.

Despite these limitations, there are several advantages to this method that make it suitable for forensic use. Although a board-certified forensic odontologist (H.F., DMD) performed all the analyses in the present study, the mathematical processes themselves are not very complicated and can be automated. Thus, these could conceivably be performed by individuals without a dental degree or license. There is no possibility to misuse the data to gain private information because this method utilizes coordinates.

The tooth sockets are likely to be maintained even if the teeth fall out because of various post-mortem changes. Thus, we focused on the positional relationships of the structures in the jaw, including the tooth sockets, between the AM and “PM” images. There have been several studies that used the Procrustes distance as a mathematical method of describing the jaw structure [16–20]. However, these papers evaluated only the Procrustes distances in their study populations. In the present study, we attempted both the Procrustes distances and Pearson's correlation coefficients. The Procrustes distance values were relatively distinct even in cases for which the correlation coefficients were similar. We could evaluate the accuracy only using the Procrustes distance.

An artificial tooth's position is not always in the original alveolar tooth socket, and it does not always have a lamina dura. Thus, we did not place landmarks on artificial tooth sockets. To increase the robustness of our results, we only compared AM cases with the same dental formula as the “PM” samples. Patients who did not have the same dental formula as the samples were thus excluded from this study (Tables 1 and 2).

To reconstruct a PMCT panoramic image from CT data, the CPR mode on the software is typically applied to each jaw separately. The axes must be positioned carefully because the bodies and jaws are not always in their standard anatomical positions. In practical forensic cases, there is a greater variation in the sharpness of the images and the markings for reconstructions can vary. Therefore, the positions of the landmarks can also vary, depending on the sharpness of the images, the X-ray equipment used, and operator error.

Furthermore, the dental panoramic X-ray images provided to forensic odontologists as AM data are often obtained long before the PM images. The possibility of changes over time need to be considered. A final visual examination is always necessary to confirm the results of the mathematical comparison.

We propose that this method could contribute to phase 2 (PM data collection) of the Interpol Disaster Victim Identification system [21]. Moreover, it could aid in the search for missing persons among those with search requests.

5. Conclusions

In the present study, we obtained positive results by using the mathematical values calculated via statistical shape analysis to compare dental panoramic X-ray images with CT panoramic images. The analysis focused on anatomical structures and not on dental work characteristics. We propose that this method could be used for DVI.

To continue working on developing the present method, we have named this procedure the IDOL method (Identification of Odontology by Landmarks on images).

Additional information

We presented a summary of this study at the 4th congress of ISFRI (International Society of Forensic Radiology and Imaging) held in Leicester, United Kingdom, in May 2015.

Acknowledgements

We would like to offer our deepest thanks to our colleagues at the Fujimoto Clinic for Oral and Maxillofacial Surgery.

This study was supported by JSPS Grants-in-Aid for Scientific Research Grant Number 26932008.

References

[1] B. Morgan, A. Alminyah, A. Cala, C. O'Donnell, D. Elliott, G. Gorincour, P. Hofman, M. Iino, Y. Makino, A. Moskata, C. Robinson, G.N. Rutty, A. Sajantila, J. Vallis, N. Woodford, K. Woźniak, M. Viner, Use of post-mortem computed tomography in Disaster Victim Identification. Positional statement of the members of the disaster victim identification working group of the international society of forensic radiology and imaging; May 2014, J. Forensic Radiol. Imaging 2 (2014) 114–116.
[2] M.J. Thali, T. Markwalder, C. Jackowski, M. Sonnenschein, R. Dirnhofer, Dental CT imaging as a screening tool for dental profiling: Advantages and limitations, J. Forensic Sci. 51 (2006) 113–119.
[3] R.E. Wood, S.L. Kogon, Dental radiology considerations in DVI incidents: a review, Forensic Sci. Int. 201 (2010) 27–32.
[4] T. Aoki, Fundamentals and applications of cutting-edge imaging technology - phase-only correlation method to support the dental personal identification, Forensic Dent. Sci. 4 (2011) 19–25 (in Japanese).
[5] A.S. Forrest, Collection and recording of radiological information for forensic purposes, Aust. Dent. J. 57 (Suppl 1) (2012) 24–32.
[6] D.G. Bouwens, L. Cevidanes, J.B. Ludlow, C. Phillips, Comparison of mesiodistal root angulation with posttreatment panoramic radiographs and cone-beam computed tomography, Am. J. Orthod. Dentofac. Orthop. 139 (2011) 126–132.
[7] V. Pinchi, G.-A. Norelli, F. Caputi, G. Fassina, F. Pradella, C. Vincenti, Dental identification by comparison of antemortem and postmortem Dental radiographs: influence of operator qualifications and cognitive bias, Forensic Sci. Int. 222 (2012) 252–255.
[8] S. Tohnak, A. Mehnert, M. Mahoney, S. Crozier, Dental identification system based on unwrapped CT images, in: Proceedings 31st Annual International Conference IEEE Eng. Med. Biol. Soc. Eng. Futur. Biomed. EMBC 2009, 2009, pp. 3549–3552.
[9] R. Dudhia, P.A. Monsour, N.W. Savage, R.J. Wilson, Accuracy of angular measurements and assessment of distortion in the mandibular third molar region on panoramic radiographs, Oral. Surg. Oral. Med. Oral. Pathol. Oral. Radiol. Endod. 111 (2011) 508–516.
[10] D.T. Van Der Meer, P.C. Brumit, B. a. Schrader, S.B. Dove, D.R. Senn, Root morphology and anatomical patterns in forensic dental identification: a comparison of computer-aided identification with traditional forensic dental identification, J. Forensic Sci. 55 (2010) 1499–1503.
[11] V. Santoro, P. Lozito, N. Mastrorocco, A. De Donno, F. Introna, Personal identification by morphometric analyses of intra-oral radiographs of unrestored teeth*, J. Forensic Sci. 54 (2009) 1081–1084.
[12] A.L. Brough, B. Morgan, S. Black, G.N. Rutty, C. Adams, Post-mortem computed tomography age assessment of juvenile dentition: comparison against traditional OPT assessment, Int. J. Leg. Med. 128 (2014) 653–658.
[13] I.L. Dryden, K.V. Mardia, Shape space and distance, in: I.L. Dryden, K.V. Mardia (Eds.), Statistical Shape Analysis, John Wiley, New York, 1998, pp. 53–82.
[14] H. Fujimoto, Inflection of Ai in the personal identity at the time of the large-scale disaster, Innervision 30 (2015) 72–74 (in Japanese).
[15] H. Fujimoto, M. Iino, The development of dental identification using reconstructed postmortem CT panoramic images, Forensic Dent. Sci. 6 (2013) 41–44 (in Japanese).
[16] M.A. Bush, P.J. Bush, H.D. Sheets, A study of multiple bitemarks inflicted in human skin by a single dentition using geometric morphometric analysis, Forensic

Sci. Int. 211 (2011) 1–8.
[17] H.D. Sheets, M.A. Bush, Mathematical matching of a dentition to bitemarks: use and evaluation of affine methods, Forensic Sci. Int. 207 (2011) 111–118.
[18] K.E. Stull, M.W. Kenyhercz, E.N. L'Abbé, Ancestry estimation in South Africa using craniometrics and geometric morphometrics, Forensic Sci. Int. 245C (2014) (206.e1–206.e7).
[19] L.J. Short, B. Khambay, A. Ayoub, C. Erolin, C. Rynn, C. Wilkinson, Validation of a computer modelled forensic facial reconstruction technique using CT data from live subjects: a pilot study, Forensic Sci. Int. 237 (2014) (147.e1–147.e8).
[20] J. Barbeito-Andrés, M. Anzelmo, F. Ventrice, M.L. Sardi, Measurement error of 3D cranial landmarks of an ontogenetic sample using computed tomography, J.Oral. Biol. Craniofacial Res. 2 (2012) 77–82.
[21] Victorian Institute of Forensic Medicine. What is DVI? Disaster Victim Identification explained. ⟨http://www.vifm.org/2014/07/what-is-dvi-disaster-victim-identification-explained/⟩, (accessed 22.06.16), 2014.